

# A Three-Channel Fluorescent Probe That Distinguishes Peroxynitrite from Hypochlorite

Quanjuan Zhang,<sup>‡</sup> Zhichuan Zhu,<sup>§</sup> Yongli Zheng,<sup>||</sup> Jiagao Cheng,<sup>‡,⊥</sup> Na Zhang,<sup>#</sup> Yi-Tao Long,<sup>#</sup> Jing Zheng,<sup>\*,§</sup> Xuhong Qian,<sup>\*,†,‡</sup> and Youjun Yang<sup>\*,†,‡</sup>

<sup>†</sup>State Key Laboratory of Bioreactor Engineering, East China University of Science and Technology, Meilong Road 130, Shanghai 200237, China

<sup>‡</sup>Shanghai Key Laboratory of Chemical Biology, <sup>§</sup>Department of Pharmaceutical Science, and <sup>⊥</sup>Shanghai Key Laboratory of New Drug Design, School of Pharmacy, East China University of Science and Technology, Meilong Road 130, Shanghai 200237, China

<sup>||</sup>School of Chemistry and Chemical Engineering, State Key Laboratory of Metal Matrix Composites, Shanghai Jiao Tong University, Dongchuan Road 800, Shanghai 200240, China

<sup>#</sup>Department of Chemistry, East China University of Science and Technology, Meilong Road 130, Shanghai 200237, China

## Supporting Information

**ABSTRACT:** A novel fluorescent probe for peroxynitrite, PN<sub>600</sub>, was rationally designed on the basis of a unique fluorophore assembly approach. PN<sub>600</sub> is a green-emitting coumarin derivative. Upon oxidation by peroxynitrite, PN<sub>600</sub> is transformed into a highly fluorescent red-emitting resorufin derivative via an orange-emitting intermediate. This three-channel signaling capability enables PN<sub>600</sub> to differentiate peroxynitrite from other reactive oxygen and nitrogen species, including hypochlorite and hydroxyl radical. Moreover, PN<sub>600</sub> is membrane-permeable and compatible with common TRITC filter sets and displays low cytotoxicity. Therefore, PN<sub>600</sub> is a promising candidate for in vitro peroxynitrite imaging.

Peroxynitrite (OONO<sup>-</sup>) was first discovered as an endogenous oxidant in 1990.<sup>1</sup> It is generated via the nearly diffusion-controlled combination of nitric oxide (NO) and superoxide radical anion. Further research revealed that it largely mediates the apparent cytotoxicity of NO.<sup>1,2</sup> OONO<sup>-</sup> can lead to protein malfunction via two distinct mechanisms: (1) nitration of the phenol moiety of tyrosine residues and (2) oxidation of a wide range of substrates, including transition-metal centers, cysteine, methionine, tryptophan, and histidine. It can also induce lipid peroxidation and DNA damage.<sup>3</sup> Cell apoptosis or necrosis often results when the cell damage from OONO<sup>-</sup> overwhelms the cell repairing capacity. Direct correlations between OONO<sup>-</sup> and numerous pathological conditions, such as cardiovascular diseases, circulatory shock, inflammation, cancers, stroke, reperfusion injury, neurodegenerative disorders, and diabetes, have been established.<sup>3f</sup> Therefore, methods for detection of cellular OONO<sup>-</sup> levels are of considerable significance for both disease diagnosis and exploration of its diverse pathophysiology.

Immunohistological quantification of cellular nitrotyrosine has been widely used to estimate the OONO<sup>-</sup> activity.<sup>4</sup> However, this approach is complicated by the presence of alternative tyrosine nitration mechanisms and lack of high spatiotemporal resolution.<sup>5</sup> Comparatively, luminescence measurements, espe-

cially fluorescence-based techniques, are advantageous and have become routine practice in the field. Reduced xanthene dyes and chemiluminescent probes are the earliest luminescent probes for OONO<sup>-</sup>. They have been frequently used despite their poor selectivity.<sup>6,7</sup> Recently, a number of small-molecule fluorescent probes for OONO<sup>-</sup> [Figure S22 in the Supporting Information (SI)] have been reported in the literature.<sup>8</sup> They are improved in many aspects compared with the reduced xanthenes and have found applications in biomedical studies.<sup>9</sup> However, optimal selectivity against highly oxidative species such as hypochlorite (ClO<sup>-</sup>) and hydroxyl radicals (HO<sup>•</sup>) still remains challenging.

Herein we describe a novel small-molecule fluorescent probe, PN<sub>600</sub>, that displays high selectivity toward OONO<sup>-</sup>. It delivers a sensitive, three-channel fluorescence signal and holds great potential in cell-imaging applications. Probes that yield signals on more than one channel are highly desirable since they enable self-calibration and circumvent complications from fluorophore photobleaching, uneven probe loading, and fluctuations of the excitation source.<sup>10</sup> To our knowledge, PN<sub>600</sub> is the first small-molecule multichannel probe for OONO<sup>-</sup>.

Our strategy for OONO<sup>-</sup> detection relies on a rationally designed oxidative coupling reaction reminiscent of phenol oxidation. The oxidation of phenol into hydroquinone involves nucleophilic attack of a cationic intermediate by H<sub>2</sub>O.<sup>11</sup> We envisioned that oxidation of a phenol with an amino group in close proximity could lead to predominant aminophenol formation due to the enhanced nucleophilicity of the amino group relative to water. Subsequent two-electron oxidation of aminophenol would give rise to an iminoquinone. On the basis of this hypothesis, we designed PN<sub>600</sub>, which bears the aforementioned structural features for detection of oxidative species and a coumarin moiety for signal transduction (Figure 1). Importantly, the coumarin moiety is installed in such a way that a resorufin derivative (2) is obtained via an oxidation-initiated cascade. Bathochromic-shifted absorption and emission bands were expected, generating a multichannel probe.

Received: May 24, 2012

Published: September 14, 2012

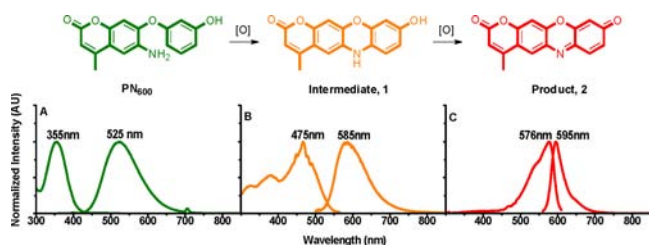


**Figure 1.** Detection scheme and normalized excitation/emission spectra of (A) PN<sub>600</sub>, (B) 1, and (C) 2. The  $\epsilon \times \phi$  of PN<sub>600</sub>, 1, and 2 were found to be  $9000 \times 0.09$  in H<sub>2</sub>O,  $17\,000 \times 0.01$  in H<sub>2</sub>O, and  $31\,000 \times 0.62$  in EtOH, respectively. The values of  $\epsilon$  are given in units of  $\text{cm}^{-1} \text{M}^{-1}$ .

PN<sub>600</sub> and intermediate 1 were synthesized and characterized (see the SI). A solution of the product, 2, which exhibits an intense purple hue and a red glow under a fluorescent lamp, was obtained by addition of a large excess (>200 equiv) of ClO<sup>-</sup> to a solution of 1 in MeOH. The molecular composition of 2 was unambiguously confirmed by high-resolution mass spectrometry ( $[M]^+ = m/z\ 279.0525$ ). Though the absorption and emission properties of this solution remained stable for days without protection from light and oxygen, compound 2 seemed to undergo reduction upon drying, and therefore, we could not isolate pure 2 for NMR characterization. The spectral and photophysical properties of PN<sub>600</sub>, 1, and 2 are included in Figure 1. The excitation maxima of PN<sub>600</sub>, 1, and 2 are widely separated from each other, while their emissions overlay at ca. 600 nm. Thus, the three species can be monitored simultaneously through their signature excitation channels at 355, 475, and 575 nm, respectively, via a single fluorescence excitation spectral scan monitored at the same emission wavelength. In these spectral studies, we chose to monitor the emission intensity at 620 nm to acquire the entire excitation band of product 2. Alternatively, 2 could be selectively excited in the presence of both PN<sub>600</sub> and 1 since its maximum excitation wavelength is much longer.

As shown by the excitation scans monitoring the emission at 620 nm (Figure 2A-1,A-2), addition of an aliquot of OONO<sup>-</sup> stock solution led to rapid consumption of probe PN<sub>600</sub> and buildup of the intermediate 1, as indicated by the excitation intensities at 350 and 467 nm, respectively. The excitation intensity of the product 2 at 575 nm also increased upon addition of OONO<sup>-</sup>; however, the signal enhancement was insignificant with additions of fewer equivalents. When the OONO<sup>-</sup> concentration exceeded 15 equiv (or 300  $\mu\text{M}$ ), the signal of the product started to rise abruptly and eventually leveled off. Concomitantly, the intermediate signal decreased. This single experiment clearly exemplifies the multichannel capability of probe PN<sub>600</sub> in OONO<sup>-</sup> detection. Alternatively, an emission scan with excitation at 550 nm could be used to monitor the formation of product selectively (Figure 2A-3,A-4). A fluorescence turn-on signal at 595 nm was observed to appear from a dark background. The fluorescence turn-on ratio was extremely high, and the detection sensitivity was optimal. Moreover, the ability to be excited efficiently at 550 nm and emit at 595 nm makes 2 an ideal fluorophore to be coupled with the widely available TRITC filter set in imaging studies, which has excitation and emission bandpasses of  $555 \pm 10$  and  $600 \pm 20$  nm, respectively.

In a parallel study (Figure 2B), it was found that ClO<sup>-</sup> could also induce oxidation of PN<sub>600</sub> to form intermediate 1. Addition of ca. 10 equiv of ClO<sup>-</sup> (or 200  $\mu\text{M}$ ) led to the total

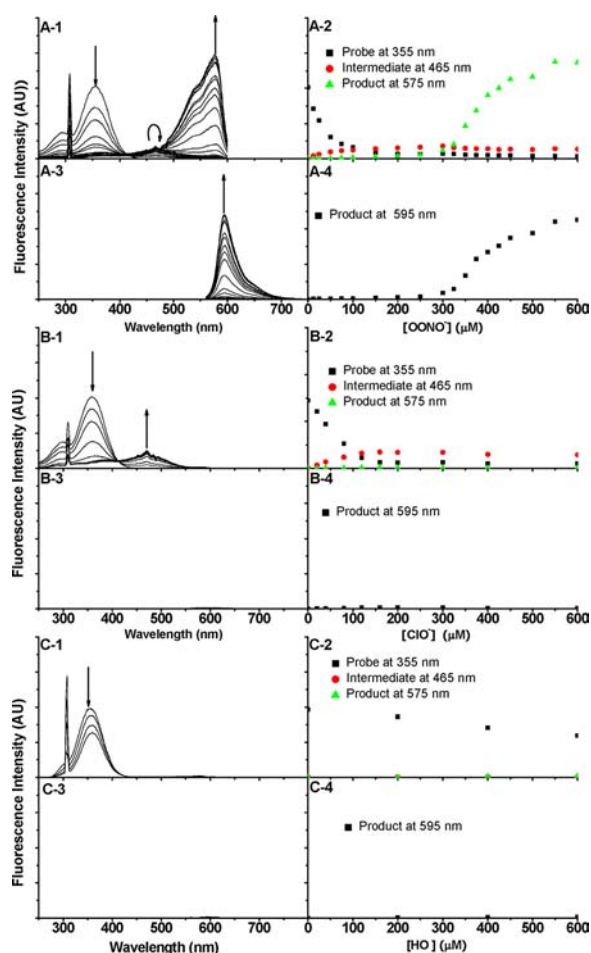


**Figure 2.** Fluorescence spectral studies of OONO<sup>-</sup>, ClO<sup>-</sup>, and HO<sup>•</sup> detection by PN<sub>600</sub> (20  $\mu\text{M}$  in 50 mM phosphate buffer at pH 7.4): (1) Excitation spectra upon addition of varying amounts of (A-1) OONO<sup>-</sup>, (B-1) ClO<sup>-</sup>, and (C-1) HO<sup>•</sup> with monitoring of the emission at 620 nm. (2) Changes in the excitation intensities at 355 nm (probe channel), 465 nm (intermediate channel), and 575 nm (product channel) with respect to the added amounts of (A-2) OONO<sup>-</sup>, (B-2) ClO<sup>-</sup>, and (C-2) HO<sup>•</sup>. (3) Emission spectra upon addition of varying amounts of (A-3) OONO<sup>-</sup>, (B-3) ClO<sup>-</sup>, and (C-3) HO<sup>•</sup> with excitation at 550 nm. (4) Changes in the emission intensity at 595 nm with respect to the added amounts of (A-4) OONO<sup>-</sup>, (B-4) ClO<sup>-</sup>, and (C-4) HO<sup>•</sup>. Spikes at 310 nm are second-order scattered light.

disappearance of the probe signal at 350 nm, and the signal intensity of 1 at 467 nm correspondingly reached a plateau. However, ClO<sup>-</sup> could not further oxidize the intermediate to form the product 2. Essentially no product excitation at 575 nm was observed with further addition of ClO<sup>-</sup> up to 30 equiv (or 600  $\mu\text{M}$ ). Both ClO<sup>-</sup> and OONO<sup>-</sup> are well-known for their high oxidizing capacities; therefore, it has been challenging to attain high degree of selectivity for one or the other of these species when developing fluorescent probes. Herein we have shown that PN<sub>600</sub> can reliably differentiate OONO<sup>-</sup> from ClO<sup>-</sup>.

We then examined the selectivity of PN<sub>600</sub> against HO<sup>•</sup>, which was generated in situ via Fenton chemistry<sup>12</sup> by mixing H<sub>2</sub>O<sub>2</sub> and Fe<sup>2+</sup>. Although HO<sup>•</sup> has been found to interfere with OONO<sup>-</sup> detection using some benchmark fluorescent probes that also contain electron-rich aromatic moieties,<sup>8b</sup> it did not interfere with PN<sub>600</sub> in our case. Addition of up to 30 equiv of Fe(ClO<sub>4</sub>)<sub>2</sub> solution into a probe solution containing a large excess of H<sub>2</sub>O<sub>2</sub> yielded only a 30% decrease of the probe signal intensity (Figure

2C). Only minimal amounts of the intermediate and the product were observed, and the signal intensities were negligible compared with those from OONO<sup>-</sup> oxidation. Attempts to introduce more Fe(ClO<sub>4</sub>)<sub>2</sub> into the solution resulted in Fe(OH)<sub>2</sub> precipitation, which led to intense light scattering.

In aqueous media or cells, OONO<sup>-</sup> can rearrange into nontoxic nitrate via H<sup>+</sup>- or CO<sub>2</sub>-catalyzed pathways; therefore, the “production rate” of OONO<sup>-</sup> in units of μM/min and the “dosage” in units of μM·min are commonly employed to complement or replace the use of “steady-state concentration”.<sup>13</sup> The physiological steady-state OONO<sup>-</sup> concentration lies between nanomolar and low micromolar,<sup>14</sup> with the cell production rate ranging from 0.1–1 μM/min<sup>15</sup> to 50–100 μM/min.<sup>3c</sup> Bolus addition of 600 μM OONO<sup>-</sup>, which is the highest concentration employed in our fluorescence titration study, is equivalent to an exposure of sustained OONO<sup>-</sup> production at a rate of 16 μM/min for 1 min or 1.6 μM/min for 10 min.<sup>13,16</sup> Therefore, the seemingly high OONO<sup>-</sup> concentration falls within the biorelevant concentration range. Additionally, bolus addition of OONO<sup>-</sup> stock solution above 1 mM is not uncommon.<sup>17</sup>

Other common reactive oxygen and nitrogen species, including hydrogen peroxide (H<sub>2</sub>O<sub>2</sub>), singlet oxygen (<sup>1</sup>O<sub>2</sub>), superoxide radical anion (O<sub>2</sub><sup>•-</sup>) and nitric oxide (NO), were found not to interfere under the same conditions (Figure 3).

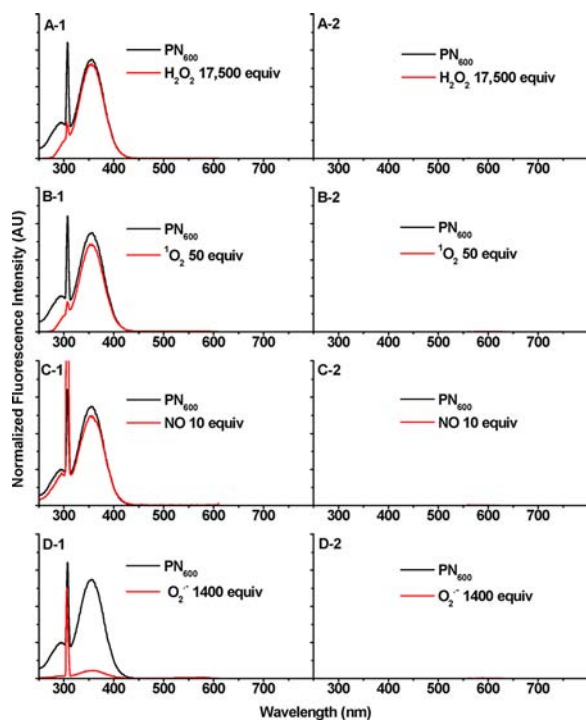


**Figure 3.** PN<sub>600</sub> selectivity studies: (1) Excitation spectra upon addition of (A-1) H<sub>2</sub>O<sub>2</sub>, (B-1) <sup>1</sup>O<sub>2</sub>, (C-1) NO, and (D-1) O<sub>2</sub><sup>•-</sup>. Emission was monitored at 620 nm. (2) Emission spectra with excitation at 550 nm upon addition of (A-2) H<sub>2</sub>O<sub>2</sub>, (B-2) <sup>1</sup>O<sub>2</sub>, (C-2) NO, and (D-2) O<sub>2</sub><sup>•-</sup>.

Bolus addition of H<sub>2</sub>O<sub>2</sub> (ca. 17 500 equiv), <sup>1</sup>O<sub>2</sub> (ca. 50 equiv), and NO (ca. 10 equiv) led to essentially no discernible spectral changes in any of the three channels for probe, intermediate, and product. The <sup>1</sup>O<sub>2</sub> was generated by addition of a ClO<sup>-</sup> stock solution into a probe solution containing a large excess of H<sub>2</sub>O<sub>2</sub>. NO in an air-saturated solution is oxidized into N<sub>2</sub>O<sub>3</sub>, which can nitrosylate aniline, and many fluorescent probes for NO,

including DAF<sup>18</sup> and NO<sub>550</sub>,<sup>19</sup> are based on this reaction. However, the amino group in PN<sub>600</sub> presumably has reduced nucleophilicity compared with that in aniline since it is attached to a rather electron-deficient coumarin core. Thus, hydrolysis of N<sub>2</sub>O<sub>3</sub> probably outcompetes the N-nitrosation. A higher dose of NO was not tested because of the low solubility of NO in H<sub>2</sub>O (~1.9 mM<sup>3f</sup>). Upon the addition of a large excess of O<sub>2</sub><sup>•-</sup> (ca. 1400 equiv in the form of solid KO<sub>2</sub>) to the probe solution with vigorous stirring, the solution fluorescence was measured 5 min after the oxygen evolution ceased. It was found that the probe signal was largely diminished with no enhancement of either the intermediate or product channel. A titration experiment showed that the UV–vis absorption of the PN<sub>600</sub> solution underwent an insignificant but consistent spectral change (Figure S24). This suggests that PN<sub>600</sub> could react with superoxide via a mechanism that is still unclear. Nevertheless, neither **1** nor **2** was observed, and hence, no interferences would result even with an extremely high dose of superoxide.

The potentials of PN<sub>600</sub> for in vitro imaging applications were examined using human glioma cell line U87. Upon addition of a PN<sub>600</sub> stock solution to the cell culture, the probe was found to cross the cell membrane readily. The presence of a phenolic hydroxyl group and an amino group did not raise any complications in regard to cell permeability, presumably because of the good separation of their pK<sub>a</sub> values (ca. 10 for OH and ca. 4.5 for NH<sub>3</sub><sup>+</sup>) from the physiological pH range (6.9–7.4), leading to the probe molecule being largely uncharged.

As expected, PN<sub>600</sub> (20 μM) did not give any background signal when imaged with the TRITC filter set (Figure 4B). This is

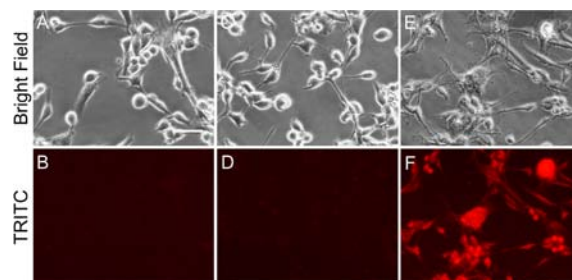


**Figure 4.** Live-cell imaging using PN<sub>600</sub>. Phase contrasts and images of human glioma cells treated with (A, B) 20 μM PN<sub>600</sub>, (C, D) 20 μM PN<sub>600</sub> + 200 μM ClO<sup>-</sup>, and (E, F) 20 μM PN<sub>600</sub> + 200 μM SIN-1 are shown. The scale bar is 50 μm.

highly desirable for imaging applications, since a fluorescence signal over a dark background renders highest possible contrast and can be captured in a sensitive and unambiguous manner. PN<sub>600</sub> did not exhibit obvious cytotoxicity at this level within 16 h, as determined by an MTT assay. Addition of ClO<sup>-</sup> (200 μM) did not lead to any detectable signal within 12 h (Figure 4D). In contrast, addition of the OONO<sup>-</sup> donor 3-morpholinosydnonimine (SIN-1) (200 μM) into cells loaded with the same level of PN<sub>600</sub> resulted in an obvious fluorescence enhancement (Figure 4F). SIN-1 provides a sustained OONO<sup>-</sup> flow in buffered aqueous media, making it a donor that well mimics the cell production of OONO<sup>-</sup>.<sup>20</sup> The maximum OONO<sup>-</sup> production rate was assayed to be ca. 1.4% of the added SIN-1 concentration.<sup>21</sup> Therefore, the use of 200 μM SIN-1 in cell-imaging studies is equivalent to treating cells with a sustained OONO<sup>-</sup> source of ca. 2.8 μM/min. Again, this is in the biorelevant range. These experiments proved that PN<sub>600</sub> has great promise for in vitro OONO<sup>-</sup> imaging applications.



In summary, we have developed PN<sub>600</sub>, a redox-active, low-molecular-weight fluorescent probe for imaging OONO<sup>-</sup>. Notably, PN<sub>600</sub> yielded a three-channel fluorescence signal upon addition of peroxyxynitrite and a dual-channel signal for hypochlorite. Other commonly occurring reactive species involved in cell oxidative burst did not interfere. The chemical structure of PN<sub>600</sub> is compact, with a molecular weight as low as 283 amu, as a result of the use of a novel probe design principle: the fluorophore for signaling is assembled in situ via a substrate-triggered chemical reaction. In addition, PN<sub>600</sub> is membrane-permeable and displays low cytotoxicity. With the aid of a routine fluorescence microscope equipped with a common TRITC filter set, PN<sub>600</sub> selectively detected peroxyxynitrite in cellular studies.

## ■ ASSOCIATED CONTENT

### Supporting Information

General methods, synthesis and characterization data, scans of original <sup>1</sup>H/<sup>13</sup>C NMR spectra and mass spectra, chemical structures and abbreviations of existing OONO<sup>-</sup> probes, UV-vis absorption titration of PN<sub>600</sub> by KO<sub>2</sub>, and cyclic voltammograms of PN<sub>600</sub> and **1**. This material is available free of charge via the Internet at <http://pubs.acs.org>.

## ■ AUTHOR INFORMATION

### Corresponding Author

youjunyang@ecust.edu.cn; xhqian@ecust.edu.cn

### Notes

The authors declare no competing financial interest.

## ■ ACKNOWLEDGMENTS

The work was supported by the State Key Laboratory of Bioreactor Engineering via the National Special Fund (2060204) and the Open Funding Project, the Fundamental Research Funds for the Central Universities (WJ1014005), the Natural Science Foundation of Shanghai Municipality (11ZR1408800), and the National Natural Science Foundation of China (21106043). We thank Prof. Yufang Xu, Prof. Weiping Zhu, and Prof. Yongfeng Zhou for insightful discussions and Dr. Mark Lowry, Dr. Michelle A. Ivy, and Prof. Wei Wang for help with manuscript preparation.

## ■ REFERENCES

- (1) Beckman, J. S.; Beckman, T. W.; Chen, J.; Marshall, P. A.; Freeman, B. A. *Proc. Natl. Acad. Sci. U.S.A.* **1990**, *87*, 1620.
- (2) (a) Radi, R.; Beckman, J. S.; Bush, K. M.; Freeman, B. A. *J. Biol. Chem.* **1991**, *266*, 4244. (b) Hogg, N.; Darley-Usmar, V. M.; Wilson, M. T.; Moncada, S. *Biochem. J.* **1992**, *281*, 419.
- (3) (a) Squadrito, G. L.; Pryor, W. A. *Free Radical Biol. Med.* **1998**, *25*, 392. (b) *Nitric Oxide Biology and Pathobiology*; Ignarro, L. J., Ed.; Academic Press: San Diego, CA, 2000. (c) Augusto, O.; Bonini, M. G.; Amanso, A. M.; Linares, E.; Santos, C. C.; de Menezes, S. L. *Free Radical Biol. Med.* **2002**, *32*, 841. (d) Alvarez, B.; Radi, R. *Amino Acids.* **2003**, *25*, 295. (e) Szabó, C.; Ischiropoulos, H.; Radi, R. *Nat. Rev. Drug Discovery* **2007**, *6*, 662. (f) Pacher, P.; Beckman, J. S.; Liaudet, L. *Physiol. Rev.* **2007**, *87*, 315.
- (4) (a) Ischiropoulos, H. *Arch. Biochem. Biophys.* **1998**, *356*, 1. (b) Radi, R. *Proc. Natl. Acad. Sci. U.S.A.* **2004**, *101*, 4003.
- (5) (a) Halliwell, B. *FEBS Lett.* **1997**, *411*, 157. (b) Eiserich, J. P.; Hristova, M.; Cross, C. E.; Jones, A. D.; Freeman, B. A.; Halliwell, B.; van der Vliet, A. *Nature* **1998**, *391*, 393. (c) van der Vliet, A.; Eiserich, J. P.; Shigenaga, M. K.; Cross, C. E. *Am. J. Respir. Crit. Care.* **1999**, *160*, 1. (d) Reiter, C. D.; Teng, R. J.; Beckman, J. S. *J. Biol. Chem.* **2000**, *275*, 32460.

- (6) (a) Kooy, N. W.; Royall, J. A.; Ischiropoulos, H.; Beckman, J. S. *Free Radical Biol. Med.* **1994**, *16*, 149. (b) Szabó, C.; Salzman, A. L.; Ischiropoulos, H. *FEBS Lett.* **1995**, *372*, 229. (c) Crow, J. P. *Nitric Oxide* **1997**, *1*, 145. (d) Possel, H.; Noack, H.; Augustin, W.; Keilhoff, G.; Wolf, G. *FEBS Lett.* **1997**, *416*, 175. (e) Kooy, N. W.; Royall, J. A.; Ischiropoulos, H. *Free Radical Res.* **1997**, *27*, 245. (f) Bonini, M. G.; Rota, C.; Tomasi, A.; Mason, R. P. *Free Radical Biol. Med.* **2006**, *40*, 968. (g) Kalyanaraman, B.; Darley-Usmar, V.; Davies, K. J.; Dennerly, P. A.; Forman, H. J.; Grisham, M. B.; Mann, G. E.; Moore, K.; Roberts, L. J.; Ischiropoulos, H. *Free Radical Biol. Med.* **2012**, *52*, 1.

- (7) (a) Radi, R.; Cosgrove, T. P.; Beckman, J. S.; Freeman, B. A. *Biochem. J.* **1993**, *290*, 51. (b) Tarpey, M. M.; Fridovich, I. *Circ. Res.* **2001**, *89*, 224. (c) Freitas, M.; Lima, J. L.; Fernandes, E. *Anal. Chim. Acta* **2009**, *649*, 8.

- (8) (a) Yang, X. F.; Guo, X. Q.; Zhao, Y. B. *Talanta* **2002**, *57*, 883. (b) Setsukinai, K.; Urano, Y.; Kakinuma, K.; Majima, H. J.; Nagano, T. *J. Biol. Chem.* **2003**, *278*, 3170. (c) Ueno, T.; Urano, Y.; Kojima, H.; Nagano, T. *J. Am. Chem. Soc.* **2006**, *128*, 10640. (d) Yang, D.; Wang, H. L.; Sun, Z. N.; Chung, N. W.; Shen, J. G. *J. Am. Chem. Soc.* **2006**, *128*, 6004. (e) Sun, Z. N.; Wang, H. L.; Liu, F. Q.; Chen, Y.; Tam, P. K.; Yang, D. *Org. Lett.* **2009**, *11*, 1887. (f) Sikora, A.; Zielonka, J.; Lopez, M.; Joseph, J.; Kalyanaraman, B. *Free Radical Biol. Med.* **2009**, *47*, 1401. (g) Peng, T.; Yang, D. *Org. Lett.* **2010**, *12*, 4932. (h) Zielonka, J.; Sikora, A.; Joseph, J.; Kalyanaraman, B. *J. Biol. Chem.* **2010**, *285*, 14210. (i) Xu, K.; Chen, H.; Tian, J.; Ding, B.; Xie, Y.; Qiang, M.; Tang, B. *Chem. Commun.* **2011**, *47*, 9468. (j) Tian, J.; Chen, H.; Zhuo, L.; Xie, Y.; Li, N.; Tang, B. *Chem.—Eur. J.* **2011**, *17*, 6626. (k) Yu, F.; Li, P.; Li, G.; Zhao, G.; Chu, T.; Han, K. *J. Am. Chem. Soc.* **2011**, *133*, 11030. (l) Song, C.; Ye, Z.; Wang, G.; Yuan, J.; Guan, Y. *Chem.—Eur. J.* **2010**, *16*, 6464.

- (9) (a) Haugland, R. P. *The Molecular Probes Handbook: A Guide to Fluorescent Probes and Labeling Technologies*, 10th ed.; Invitrogen: Carlsbad, CA, 2005. (b) Gaupels, F.; Spiazzi-Vandelle, E.; Yang, D.; Delledonne, M. *Nitric Oxide* **2011**, *25*, 222. (c) Ieda, N.; Nakagawa, H.; Horinouchi, T.; Peng, T.; Yang, D.; Tsumoto, H.; Suzuki, T.; Fukuhara, K.; Miyata, N. *Chem. Commun.* **2011**, *47*, 6449.

- (10) Demchenko, A. P. *J. Fluoresc.* **2010**, *20*, 1099.
- (11) Yamamura, S. *The Oxidation of Phenols*. In *The Chemistry of Phenols*; Rappoport, Z., Ed.; Wiley: New York, 2003.

- (12) Fenton, H. J. H. *J. Chem. Soc., Trans.* **1894**, *65*, 899.

- (13) Beckman, J. S.; Chen, J.; Ischiropoulos, H.; Crow, J. P. *Methods Enzymol.* **1994**, *223*, 229.

- (14) Liu, P.; Xu, B.; Quilley, J.; Wong, P. Y. *Am. J. Physiol.: Cell Physiol.* **2000**, *279*, C1970.

- (15) Supinski, G.; Stofan, D.; Callahan, L. A.; Nethery, D.; Nosek, T. M.; DiMarco, A. *J. Appl. Physiol.* **1999**, *87*, 783.

- (16) Fici, G. J.; Althaus, J. S.; von Voigtlander, P. F. *Free Radical Biol. Med.* **1997**, *22*, 223.

- (17) (a) Villa, L. M.; Salas, E.; Darley-Usmar, V. M.; Radomski, M. W.; Moncada, S. *Proc. Natl. Acad. Sci. U.S.A.* **1994**, *91*, 12383. (b) Estévez, A. G.; Radi, R.; Barbeito, L.; Shin, J. T.; Thompson, J. A.; Beckman, J. S. *J. Neurochem.* **1995**, *65*, 1543. (c) Tommasini, I.; Sestili, P.; Cantoni, O. *Mol. Pharmacol.* **2002**, *61*, 870. (d) Shacka, J. J.; Sahawneh, M. A.; Gonzalez, J. D.; Ye, Y. Z.; D'Alessandro, T. L.; Estévez, A. G. *Cell Death Differ.* **2006**, *13*, 1506.

- (18) Kojima, H.; Nakatsubo, N.; Kikuchi, K.; Kawahara, S.; Kirino, Y.; Nagoshi, H.; Hirata, Y.; Nagano, T. *Anal. Chem.* **1998**, *70*, 2446.

- (19) Yang, Y.; Seidlits, S. K.; Adams, M. M.; Lynch, V. M.; Schmidt, C. E.; Anslyn, E. V.; Shear, J. B. *J. Am. Chem. Soc.* **2010**, *132*, 13114.

- (20) Ma, X. L.; Lopez, B. L.; Liu, G. L.; Christopher, T. A.; Ischiropoulos, H. *Cardiovasc. Res.* **1997**, *36*, 195.

- (21) (a) Supinski, G.; Stofan, D.; Callahan, L. A.; Nethery, D.; Nosek, T. M.; DiMarco, A. *J. Appl. Physiol.* **1999**, *87*, 783. (b) Martín-Romero, F. J.; Gutiérrez-Martín, Y.; Henao, F.; Gutiérrez-Merino, C. *J. Fluoresc.* **2004**, *14*, 17.